3
Single-interface modes in the microwave regime

Tables

Item	Topic	Chapter 3	Chapter 4	Chapter 5	Chapter 6	Chapter 7
1	Interfaces	1	1	2	1	2
2	Types	ENG,DNG	DPS,ENG,DNG, MNG	DPS,ENG,DNG, MNG	ENG	ENG
3	ϵ_r, μ_r	complex	real	real	complex	complex
4	Dispersion	yes	no	no	no	no
5	Free β	yes	yes	yes	yes	yes
6	Loaded β	yes	no	no	yes	yes
7	Configuration	O,K	free	free	O,K	G
8	$\mathcal{R}$	yes	no	no	yes	yes
9	G–H	yes	no	no	no	no
10	E and H	no	yes	yes	yes	yes
11	S_z	no	yes	yes	yes	yes
12	S_x	no	no	no	yes	yes
13	η	yes	no	no	yes	yes
14	v_{ph} and v_{group}	yes	no	no	no	no
15	Charge density	no	no	no	yes	yes

Table 2.10. List of topics investigated in chapters 3-7.

Item	Topic	Chapter 3
1	Interfaces	1
2	Types	ENG,DNG
3	ϵ_r, μ_r	complex
4	Dispersion	yes
5	Free β	yes
6	Loaded β	yes
7	Configuration	O,K
8	$\mathcal{R}$	yes
9	G–H	yes
10	E and H	no
11	s_z	no
12	s_x	no
13	η	yes
14	v_{ph} and v_{group}	yes
15	Charge density	no

Table 3.1. List of topics investigated in this chapter.

F	f_0 (GHz)	f_μ (GHz)	f_p (GHz)
0.56	4.	6.03023	10.

Table 3.2. The parameters F, f_0 and f_p appearing in Eqs. (2.61) and (2.62), where f_μ is the frequency at which μ_r vanishes.

case	Loss	γ/f_p	Γ/f_0
(a)	Lossless	0	0
(b)	Moderately lossy	0.01	0.01
(c)	Highly lossy	0.03	0.03

Table 3.3. Relative loss (damping) parameters, γ/f_p and Γ/f_0, associated with ϵ_m and μ_m, respectively, for (a) lossless, (b) moderately lossy and (c) highly lossy metamaterials.

f (GHz)	ϵ_m	μ_m	n_m	r_m	ϕ_m (deg)
4.4	−4.16529	−2.22667	−3.04544	4.7231	208.128

Table 3.4. Values of ϵ_m, μ_m and n_m at a frequency f = 4.4 GHz, and their related radius, r_m, and angle, ϕ_m, in an ϵ_r'-μ_r' parameter space.

	f [GHz]	Limits
(b)	4.	$\mu_m \rightarrow -\infty$
(c)	4.71405	$\mu_m \rightarrow -1$
(d)	5.20102	$\beta_{TE} \rightarrow \beta_{TM}$
(e)	7.07107	$\epsilon_m \rightarrow -1$

Table 3.5. The frequencies describing the horizontal lines (b) - (d) in Fig. 3.6, associated with the asymptotic value of ϵ_m and μ_m.

Mode	TM(1)	TE	TM(2)
Type	ENG	DNG	ENG
f(GHz)	3.57136	5.07339	6.0456
ϵ_m	-6.84029	-2.88511	-1.73603
μ_m	3.20086	-0.479984	0.00397536
n_m	4.67919 i	-1.17678	0.0830743 i
r_m	7.55216	2.92476	1.73604
ϕ_m	154.923	189.446	179.869

Table 3.6. The TE, TM(1) and TM(2) modes: Media type, frequency of excitation, value of ϵ_m, μ_m, n_m, r_m and ϕ_m.

f (GHz)	Mode	Type	v_{phase}/c	v_{group}/c
3.57136	TM(1)	ENG	0.806222	0.300724
5.07339	TE	DNG	0.998469	-0.146865
6.0456	TM(2)	ENG	0.828664	0.286238

Table 3.7. Relative phase and group velocities, v_{phase}/c and v_{group}/c, respectively, for the TE, TM(1) and TM(2) modes, where c is the speed of light in free space.

f (GHz)	Mode	Type	η_c/η_0	η_m/η_0
3.57136	TM(1)	ENG	1.24035	-0.184685
5.07339	TE	DNG	0.998469	-0.371025
6.0456	TM(2)	ENG	1.20676	-0.678803

Table 3.8. Frequency, mode, media type, and relative cover and metamaterial impedance, η_c/η_0 and η_m/η_0, respectively, where η_c and η_0 are the impedance of the cover and free space, respectively.

Figures

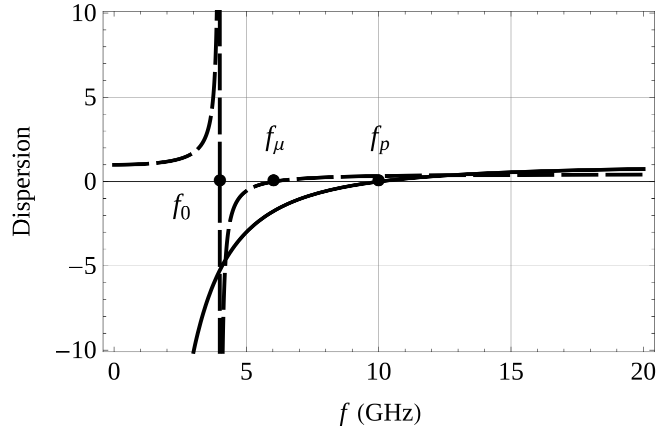

Fig. 3.1. Dispersion of ϵ_m (solid line) and μ_m (dashed line) as a function of frequency, *f*. The dots denote the frequencies at which ϵ_m and μ_m switch sign.

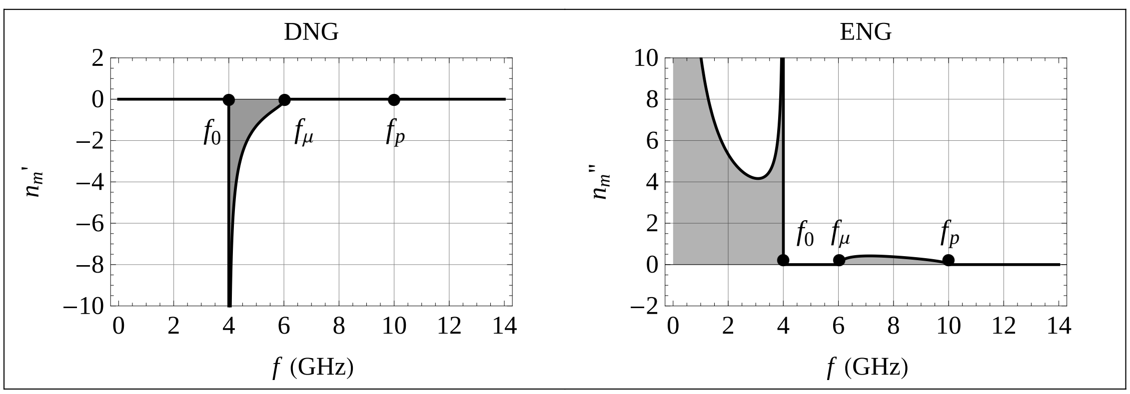

Fig. 3.2. Dispersion of n_m' and n_m'' as a function of frequency, *f*, where the dots are as in Fig. 3.1.

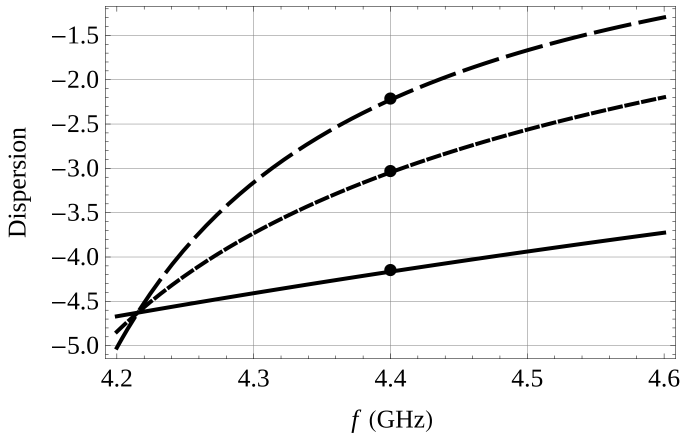

Fig. 3.3. Dispersion of ϵ_m, μ_m and n_m in a narrow frequency range where all three are negative, and their value at f = 4.4 GHz are depicted by the dots.

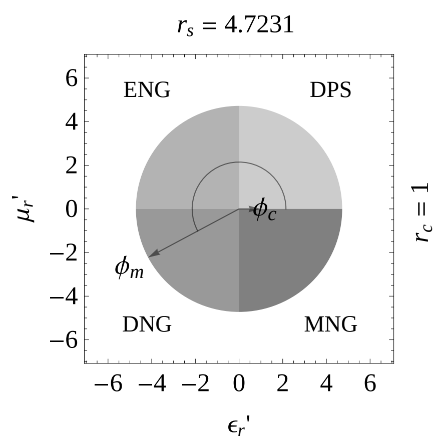

Fig. 3.4. Metamaterial type at a frequency f = 4.4 GHz, described in an ϵ_r'-μ_r' parameter space by the vector r_m and angle ϕ_m, pointing in the DNG quadrant.

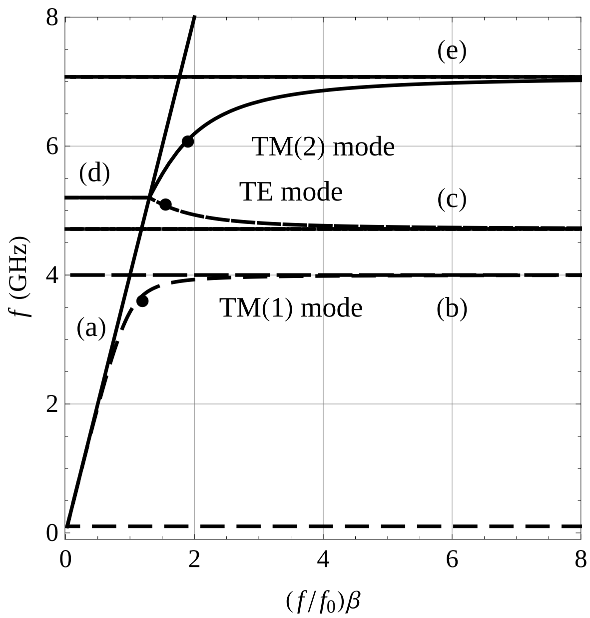

Fig. 3.6. The dispersion of the propagation constant of a single-interface mode, β, propagating along the interface separating a metamaterial and DPS-type cover. The dots represent the frequencies associated with the TE, TM(1) and TM(2) modes that could be excited by a prism at an angle θ_p = 45 deg. The lines denoted by (a) - (e) are discussed in the text.

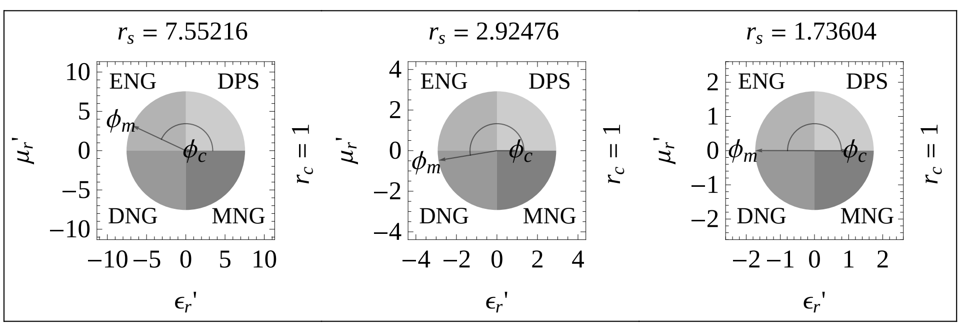

Fig. 3.7. Type of the TM(1), TE and TM(2) modes and their associated radii r_m and r_c, and angles ϕ_m and ϕ_c, in an ϵ_r'-μ_r' parameter space. Here, (left) the TM(1) mode belongs to the ENG-type metamaterial, (center) the TE mode belongs to the MNG-type metamaterial and (right) the TM(2) mode belongs to the ENG-type metamaterial.

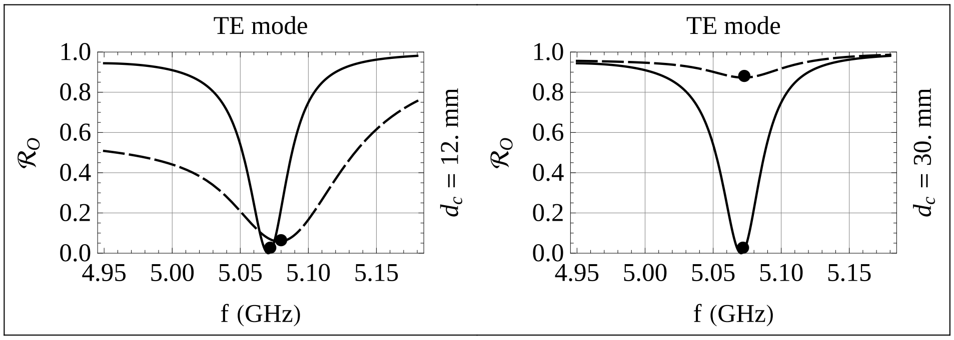

Fig. 3.10(b). The $\mathcal{L}$-spectrum (solid line) together with the $\mathcal{R}_O$-spectrum (dashed line) as a function of frequency, *f*, for (left) d_c = 12 mm and (right) 30 mm.

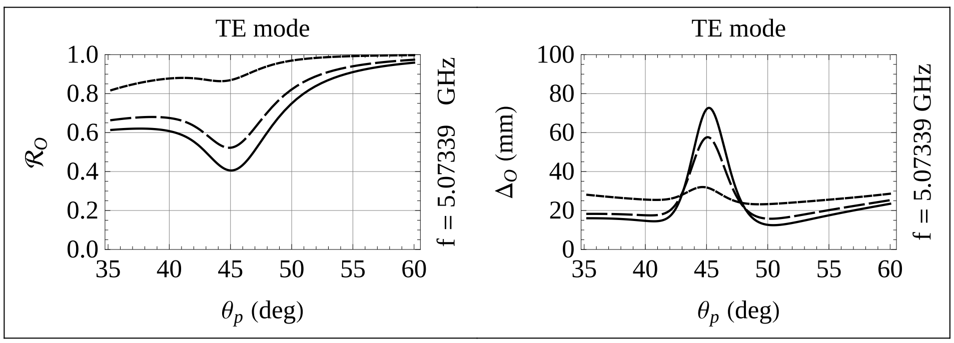

Fig. 3.10(c). (left) The $\mathcal{R}_O$-spectrum and (right) Δ_O-spectrum as a function of θ_p, both for d_c = 18 mm (solid line), 20 mm (dashed line) and 30 mm (dotted line).

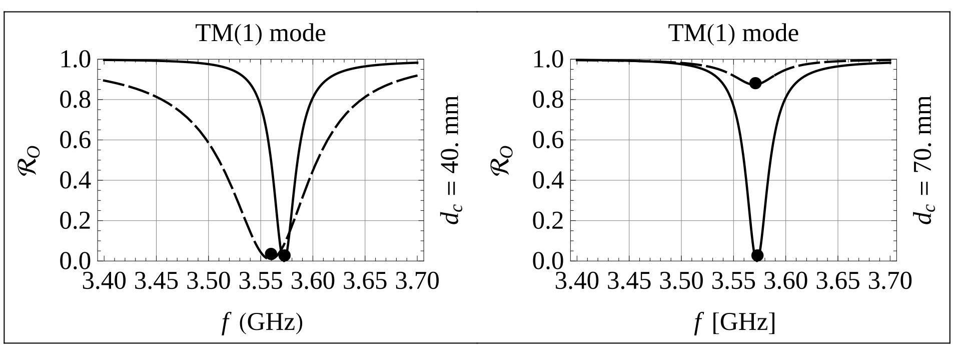

Fig. 3.11(b). The $\mathcal{L}$-spectrum (solid line) together with the $\mathcal{R}_O$-spectrum (dashed line) as a function of frequency, *f*, for (left) d_c = 40 mm and (right) 70 mm.

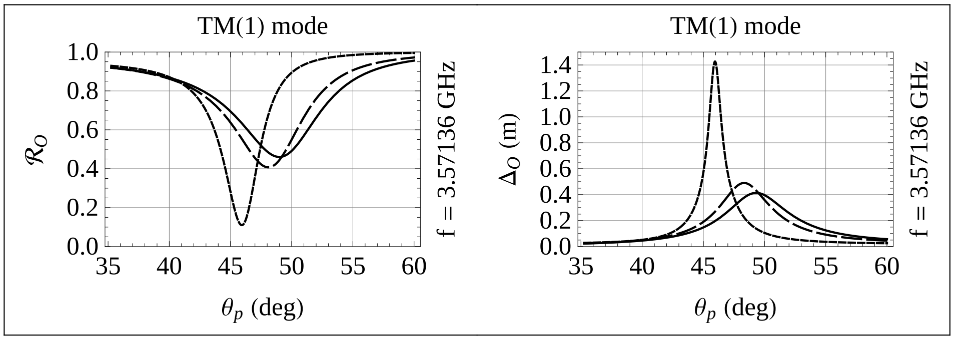

Fig. 3.11(c). The (left) $\mathcal{R}_O$-spectrum and (right) Δ_O-spectrum as a function of θ_p, both for d_c = 18 mm (solid line), 20 mm (dashed line) and 30 mm (dotted line).

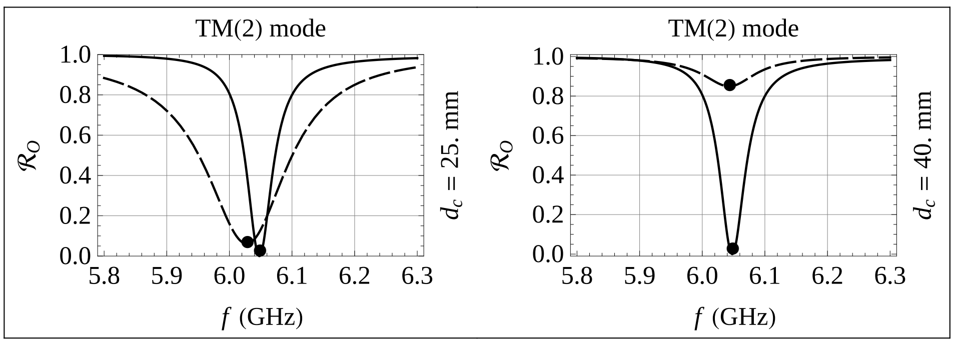

Fig. 3.12(b). The $\mathcal{L}$-spectrum (solid line) together with the $\mathcal{R}_O$-spectrum (dashed line) as a function of frequency, f, for (left) d_c = 15 mm and (right) 25 mm.

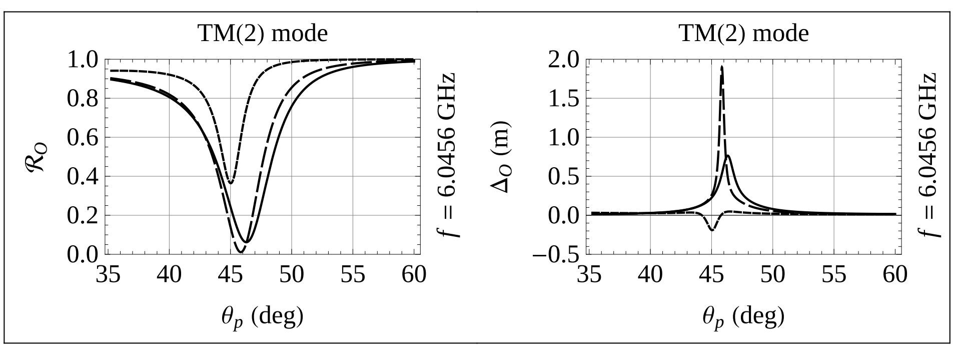

Fig. 3.12(c). (left) The $\mathcal{R}_O$-spectrum and (right) the Δ_O-spectrum as a function of θ_p, both for d_c = 18 mm (solid line), 20 mm (dashed line) and 30 mm (dotted line).

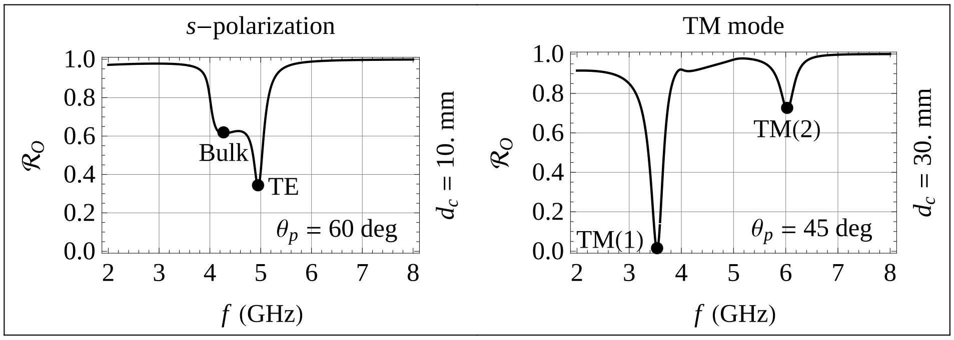

Fig. 3.13. The $\mathcal{R}_O$-spectrum for the Otto configuration as a function of frequency, f, for a TE mode with d_c = 10 mm and θ_p = 60 deg (left), and for a TM mode with d_c = 30 mm and θ_p = 45 deg (right). One observes the positions of the resonances belonging to the bulk and TE modes on the left. The resonances belonging to the TM(1) and TM(2) modes are observed on the right, but the bulk mode is barely observed.

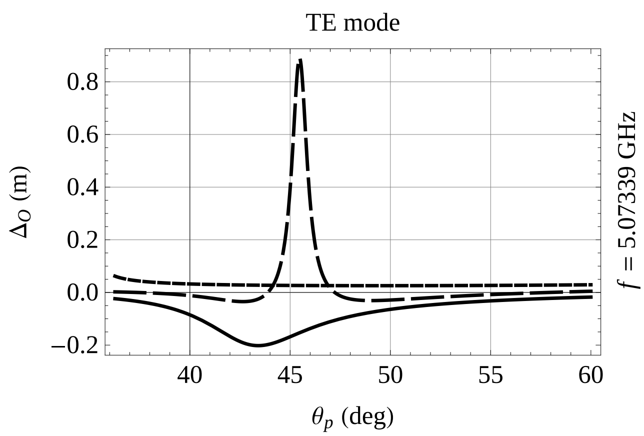

Fig. 3.14. The Δ_O-spectrum as a function of θ_p for $f = f_{\rm TE}$ and d_c = 5 mm (solid line), d_c = 10 mm (dashed line) and (c) $d_c \to \infty$ (dotted line).

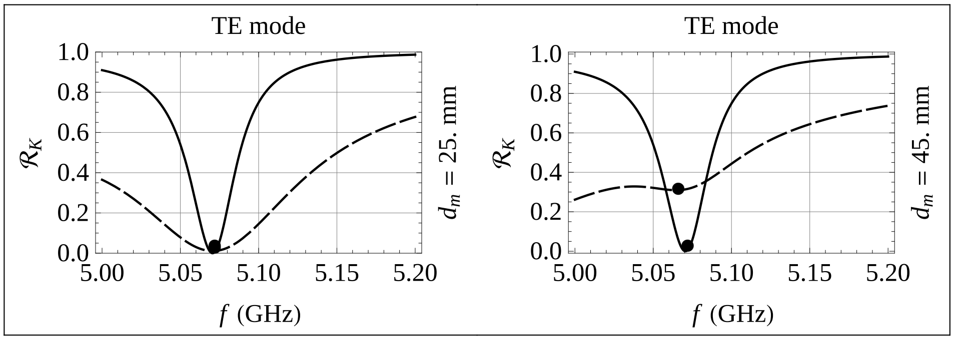

Fig. 3.16(b). The $\mathcal{L}$-spectrum (solid line) together with the $\mathcal{R}_K$-spectrum (dashed line) as a function of frequency, f, for (left) d_c = 25 mm and (right) 40.5 mm.

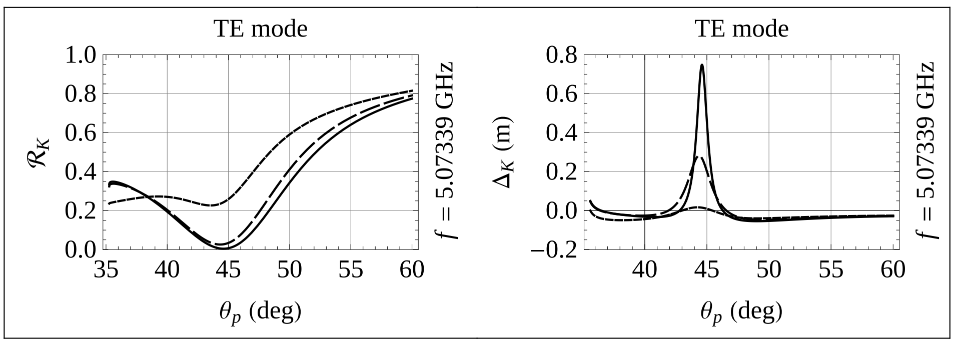

Fig. 3.16(c). (left) The $\mathcal{R}_K$-spectrum and (right) the Δ_K-spectrum as a function of θ_p, both for d_c = 24.3 mm (solid line), 27 mm (dashed line) and 45 mm (dotted line).

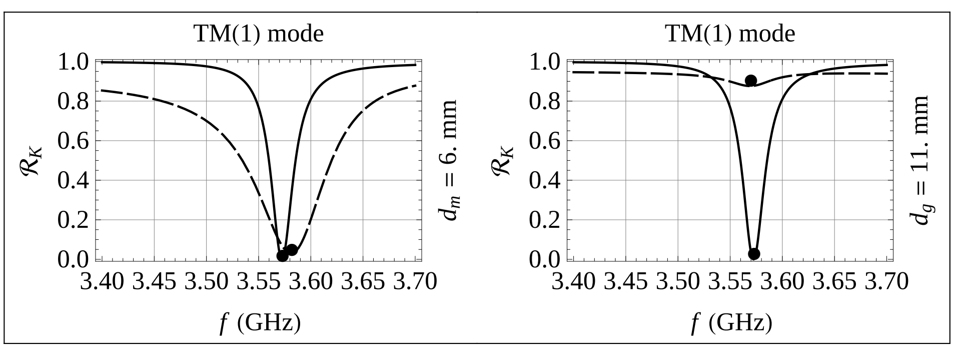

Fig. 3.17(b). The $\mathcal{L}$-spectrum (solid line) together with the $\mathcal{R}_K$-spectrum (dashed line) as a function of frequency, f, for (left) d_c = 6 mm and (right) 11 mm.

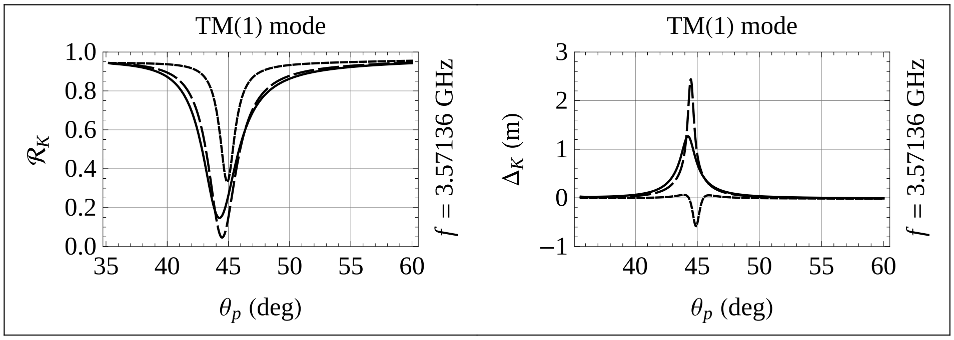

Fig. 3.17(c). (left) The $\mathcal{R}_K$-spectrum and (right) Δ_K-spectrum as a function of θ_p, both for d_c = 4.5 mm (solid line), 5 mm (dashed line) and 7.5 mm (dotted line).

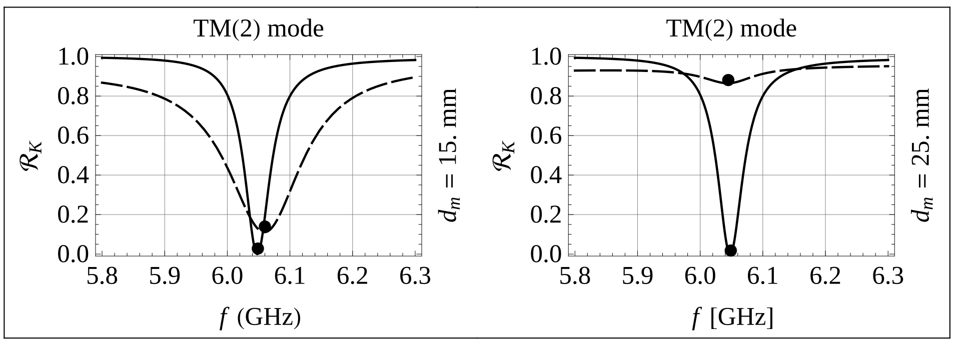

Fig. 3.18(b). $\mathcal{L}$-spectrum (solid line) together with the $\mathcal{R}_K$-spectrum (dashed line) as a function of frequency, f, for (left) d_c = 15 mm and (right) 25 mm.

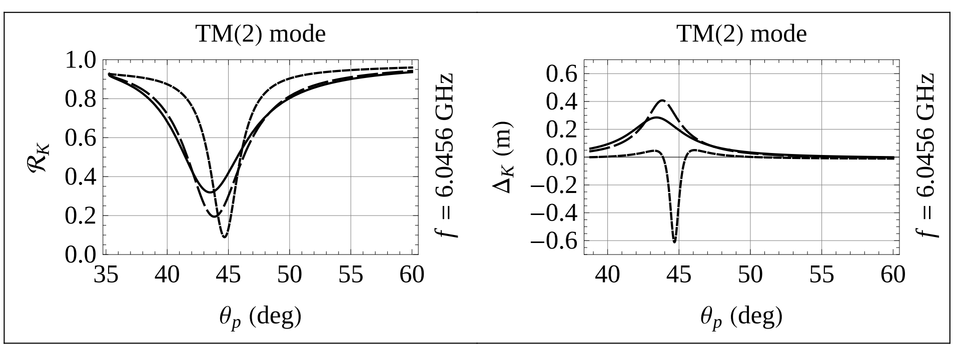

Fig. 3.18(c). (left) $\mathcal{R}_K$-spectrum and (right) Δ_K-spectrum as a function of θ_p, both for d_c = 9 mm (solid line), 10 mm (dashed line) and 15 mm (dotted line).

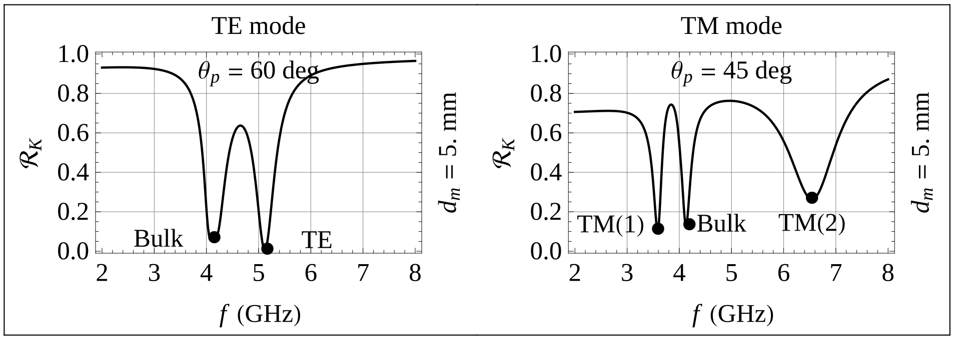

Fig. 3.19. The *s*-polarized $\mathcal{R}_K$-spectrum as a function of frequency, f, for d_m = 5 mm and θ_p = 60 deg (left), and *p*-polarized $\mathcal{R}_K$-spectrum for d_m = 5 mm and θ_p = 45 deg (right). One observes the positions belonging to the bulk and TE modes on the left. The TM(1), bulk and TM(2) modes are all clearly observed on the right.

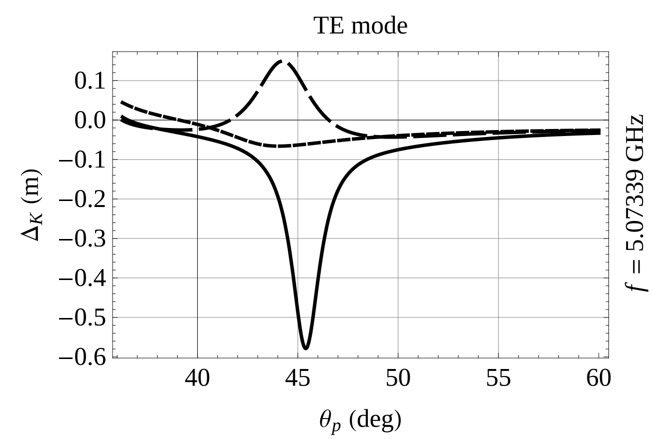

Fig. 3.20. The Δ_K-spectrum as a function of θ_p for $f = f_{TE}$ and d_c = 20 mm (solid line), d_c = 30 mm (dashed line) and (c) $d_c \to \infty$ (dotted line).

Exercises

(1) Table 3.1 includes only a partial list of the topics included in Table 2.2. Try addressing all the rest of the topics using the model metamaterial of this chapter.

(2) Discuss the meaning of charge density waves in a DNG-type medium.

(3) Compare the advantages and disadvantages of using the Otto and Kretschmann configurations.

References

[1] V. Veselago, L. Braginsky, V. Shklover and C. Hafner. Negative refractive index materials. *J. Comput. Theor. Nanosci.* **3** (2006) 2.

[2] J. B. Pendry and D. R. Smith. Reversing light with negative refraction. *Phys. Today* **57** June (2004).

[3] V. M. Agranovich, Y. R. Shen, R. H. Baughman and A. a. Zakhidov. Linear and nonlinear wave propagation in negative refraction metamaterials. *Phys. Rev. B* **69** (2004) 165112.

[4] G. Dolling, C. Enkrich, M. Wegener, C. M. Soukoulis and S. Linden. Simultaneous negative phase and group velocity of light in a metamaterial. *Science* **312** (2006) 892.

[5] H. Raether. *Surface Plasmons on Smooth and Rough Surfaces and on Gratings* (Springer Tracts in Modern Physics, Vol. 111, New York, Springer-Verlag, 1988).

[6] R. Ruppin. Surface polaritons of a left-handed medium. *Phys. Lett.* **277** (2000) 61.

[7] H. – F.Zhang, Q. Wang, N. – H.Shen, R. Li, J. Chen, J. Ding and H. – T.Wang. Surface plasmon polaritons at interfaces associated with artificial composite materials. *J. Opt. Soc. Am. B* **22** (2005) 12.

[8] T. Tamir Ed. *Integrated Optics (Topics in Applied Physics)* (Springer-Verlag, 1975).

[9] I. V. Shadrivov, A. A. Zharov and Y. S. Kivshar. Giant Goos-Hä nchen effect at the reflection from left-handed metamaterials. *Appl. Phys. Lett.* **83** (2003) 13.

[10] M. Merano, A. Aiello, G. W. ‘ tHooft, M. P. van Exter, E. R. Eliel and J. P. Woerdman. Observation of Goos- Hä nchen shifts in metallic reflection. *Opt. Exp.* **15** (2007) 24.

[11] I. V. Lindell, S. A. Tretyakov, K. I. Nikoskinen and S. Ilvonen. BW media – media with negative parameters, capable of supporting backward waves. *Micr. and Opt. Tech. Lett.* **31** (2001) 2.

[12] D. F. Nelson. Generalizing the poynting vector. *Phys. Rev. Lett.* **76** (1996) 25.

[13] J. Wuenschell and H. K. Kim. Surface plasmon dynamics in an isolated metallic nanoslit. *Optics Express* **14** (2006) 1000.